V European Conference on Computational Fluid Dynamics
ECCOMAS CFD 2010
J. C. F. Pereira and A. Sequeira (Eds)
Lisbon, Portugal,14-17 June 2010

GEOMETRY OPTIMIZATION FOR QUASI-UNIFORM FLOWS FROM SUPERSONIC NOZZLES

D. Pasquale[*], J. Harinck[⋆], A. Guardone[†] and S. Rebay[*]

[*]Dipartimento di Ingegneria Meccanica, Università di Brescia
Via Branze, 38, 25123 Brescia, Italy, e-mail: david.pasquale@ing.unibs.it

[⋆]Process and Energy Department, Delft University of Technology
Mekelweg, 2, 2828 CD Delft, The Netherlands, e-mail: j.harinck@tudelft.nl

[†]Dipartimento di Ingegneria Aerospaziale, Politecnico di Milano
Via La Masa, 34, 20156 Milano, Italy, e-mail: guardone@aero.polimi.it

Key words: Optimization, B-spline, Compressible flows, Subsonic-Supersonic nozzles

Abstract.

Gasdynamic nozzles with supersonic outflow are used in many applications, such as propulsion systems, turbines, supersonic wind tunnels and mixing devices. The standard procedure to design supersonic nozzles which produces uniform outlet flows is based on the Method Of Characteristics (MOC). This study aims to gain understanding on how a reduction in nozzle length with respect to that obtained with the MOC procedure deteriorates the outflow uniformity for a given discharge Mach number. To achieve this purpose, a global optimization method based on a Genetic Algorithm and a Computational Fluid Dynamic solver is adopted. The optimization problem is formulated in terms of three objective functions, namely, nozzle length minimization and uniform Mach number and zero velocity angle at the exit section. The flow is modelled as an inviscid flow of nitrogen expanding in a two-dimensional planar nozzle. The results include two- and three-dimensional Pareto-fronts and selected examples of Pareto-optimal nozzle designs which are compared to the MOC geometry.

1 INTRODUCTION

Gasdynamic subsonic-supersonic nozzles are used in e.g. rockets,[1] turbines,[2] supersonic wind tunnels,[3] mixing devices and molecular beams. Small nozzle lengths with rapid expansion are preferred for rockets in order to minimize weight; these are e.g. minimum length or spike nozzles. In contrast, supersonic nozzles with gently curved expansion sections are normally used in wind tunnels where high quality uniform flow is desired in the test section. Hence, wind tunnel nozzles are usually long with a relatively slow expansion. The boundary layer can therefore represent a limiting issue for these applications. This paper is concerned with supersonic nozzles that produce uniform outflow. In particular, it is motivated by the design of an organic-fluid wind tunnel that is being designed and built at the Politecnico di Milano in Italy to test total pressure probes and blade cascades.

The design of subsonic-supersonic nozzles is usually carried out using the well-known Method Of Characteristics (MOC).[4] In this method, the hyperbolic partial differential equations that govern isentropic supersonic flow are reduced to ordinary differential equations along so-called characteristic lines that emanate from a given initial line.[5] The MOC method is available for both ideal and real gas flows governed by arbitrary equations of state.[6,7]

One of the limitations of the MOC is that characteristic lines only exist in supersonic flow regimes and the method can therefore only be used for the design of the supersonic nozzle section downstream of the throat. This is not a serious problem for the design of uniform outflow nozzles, because the uniformity of the outlet flow is much more sensitive to the shape of the supersonic part rather than to the subsonic part upstream of the throat section. A second drawback is that this method reveals no information regarding the trade-off between the two design objectives uniform outflow and minimal nozzle length, and the latter strongly affects the boundary layer thickness and, therefore, the quality of nozzle outflow. A further limitation of the MOC is that it cannot be extended to viscous flows.

The present work aims at understanding the trade-off between the reduction in length of the nozzle and the outflow uniformity, in terms of magnitude and direction of the flow, for a given discharge Mach number. To this purpose, a global optimization method based on a Genetic Algorithm (GA) and a Computational Fluid Dynamic (CFD) solver is used. GAs have proven to be robust methods for global optimization of numerous fluid dynamic designs, as well as other applications. The major advantage over the MOC is that Genetic Algorithms allow for multiple objectives to be taken into consideration, and that, moreover, they also produce information regarding the trade-off between the objectives, which is effectively represented by means of a Pareto front. Furthermore, such optimization methods allow for the design of the subsonic nozzle section as well and can be easily extended to viscous flows with accurate thermodynamic and transport property models. In the present work, viscous effect are not taken into account and the Euler equations have therefore been used to compute the flow field. The reference design Mach

number of the experiment is 2, and a preliminary design using the MOC has been carried out for comparisons and for providing the initial guess to the optimization process.

The organization of the paper is as follows. Section 2 describes the methodology used for the nozzle shape parametrization, the formulation of the optimization problem and gives some details of the flow solver and grid generator used. Section 3 present results on the trade-off between design objectives for a given discharge Mach number and Section 4 contains the conclusions of the work.

2 METHODOLOGY

2.1 Geometry Parametrization

A nozzle with a rectangular cross-sectional area is considered, so that the flow field is symmetric with respect to the x-axis. The geometry of the upper-half of the nozzle is shown in Figure 1. The fluid enters from the left boundary and exits from the right one. The lower boundary is the axis of symmetry, and the upper curved boundary is the solid wall. The constrained optimization problem of interest here can be formulated either as a

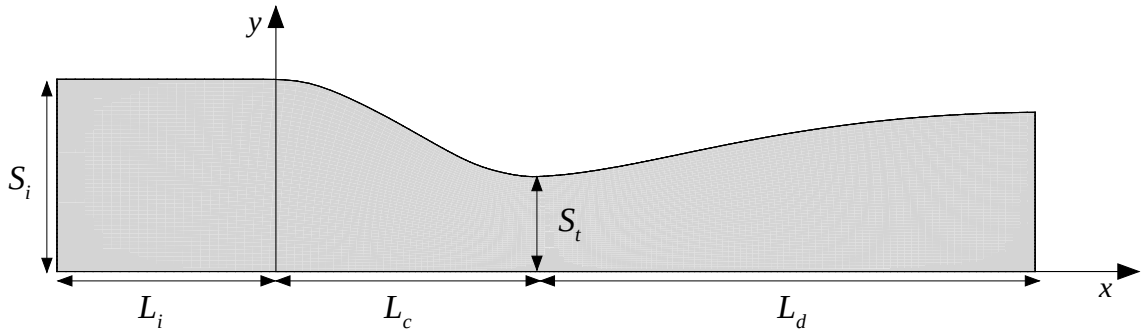

Figure 1: Upper-half of the nozzle with a rectangular cross-sectional area. The flow field is symmetric with respect to the x-axis.

minimization problem for the nozzle length at constant throat area, or equivalently as a throat area maximization problem for a constant nozzle length. Herein, the nozzle length is fixed to unity, and all important quantities that are needed to parametrize the shape, e.g., inflow span S_i and throat location L_c, are made dimensionless with respect to the throat span S_t.

The converging-diverging wall shape of the nozzle is represented by cubic B-spline curves, which are briefly presented in the following.

A B-spline curve $\mathbf{B}(u)$ of degree p can in general be written as

$$\mathbf{B}(u) = \sum_{i=0}^{n} N_{i,p}(u)\mathbf{P}_i \,,$$

where $\mathbf{P}_i$ is one of the $n+1$ control points and $n \geq p$, $N_{i,p}$ are basis function. The parameter u varies on the interval $[u_0, u_m]$; u_0 and u_m are the first and the last elements of a strictly increasing sequence of $m+1$ so-called knots, respectively. The number of control points, the degree of the curve and the number of knots are related to one another by the relation

$$m = n + p + 1\,.$$

For example, for a cubic B-spline, i.e. $p = 3$, the minimum number of control points is $n + 1 = 4$, and the corresponding number of knots is $m = n + p + 1 = 8$.

To completely define a curve, the knot sequence also has to be fixed. In general, for a given set of control points, it is difficult to judge which knot sequence is the best choice. The easiest option is to choose a uniform spacing, which is however too rigid in many cases. As a rule of thumb, better results in terms of curve smoothness are obtained if the control point location is somehow reflected in the knot sequence. In this work the knot sequence is computed by a *chordal* parametrization. A full account of the theory of B-spline curves and of the problem of parametrization can be found in many references, e.g.[8–10]

In this work, the solid wall of the nozzle is represented as a composition of two consecutive cubic B-spline curves. The first curve, $\mathbf{B}_{\mathrm{c}}(u)$, is used for the converging part and it ends at the throat area location $\mathbf{T} = (L_{\mathrm{c}}, S_{\mathrm{t}})$. The other curve, $\mathbf{B}_{\mathrm{d}}(u)$, represents the diverging part. These curves are defined by $n_{\mathrm{c}} + 1$ and $n_{\mathrm{d}} + 1$ number of points, respectively, and the shape of the upper wall is controlled by the position of the control points for both curves. Moreover, at the throat location, a fixed curvature value can be imposed preserving the C^2 continuity between the two curves if some additional constraints around the junction point are satisfied. In the case of cubic curves, these conditions concern only the two adjacent control points and the spacing of the first two different knots for both curves. As shown in Figure 3, in order to avoid any influence by the inflow boundary condition on the computed flow field, an additional straight part of the same length of the inflow span S_{i} has been added upstream of the nozzle inlet.

Up to the throat section, the shape of the nozzle does not change during the optimization process and a reasonable shape has been chosen which guarantees a smooth and gradual acceleration of the flow. The area ratio between the inflow and the throat has been chosen such that the inlet Mach number has a value of 0.3. All the quantities required to define the converging portion of the nozzle have been chosen as a fixed multiple of the throat span S_{t}, i.e., $L_{\mathrm{c}} = 3S_{\mathrm{t}}$ and $S_{\mathrm{i}} = 2.69S_{\mathrm{t}}$. Therefore, the convergent section is fixed in all computations.

The shape of the diverging part of the nozzle is controlled by the position of the unconstrained control points $\mathbf{P}_i = (x_i, y_i)$. whose, only the y-components y_i are used as design variables during the optimization process. The x-components x_i are instead fixed

along the diverging part of the nozzle according to two possible relations, i.e.,

$$x_{i+3} = L_\mathrm{t} + \left(\frac{1 - L_\mathrm{c}}{n_\mathrm{d} - 2} i\right) , \tag{1}$$

$$x_{i+3} = L_\mathrm{t} + (1 - L_\mathrm{c}) \cos\left(\frac{90}{n_\mathrm{d} - 2} i\right) , \tag{2}$$

where $0 \leq i \leq n_\mathrm{d} - 2$.

In Figure 2 the root mean square difference σ between the diverging B-spline curve and the geometry generated by the method of characteristics is plotted. For the prescribed outflow Mach number of 2, the influence of the number of control points and the type of distribution is shown. As shown in Figure 2, for both distributions, using more than 4 control points does not give substantially better results. Consequently, to limit the number of optimization parameters, the y-coordinates of four control points are chosen to represent the diverging part of the nozzle geometry and the trigonometric distribution of x-coordinates is adopted.

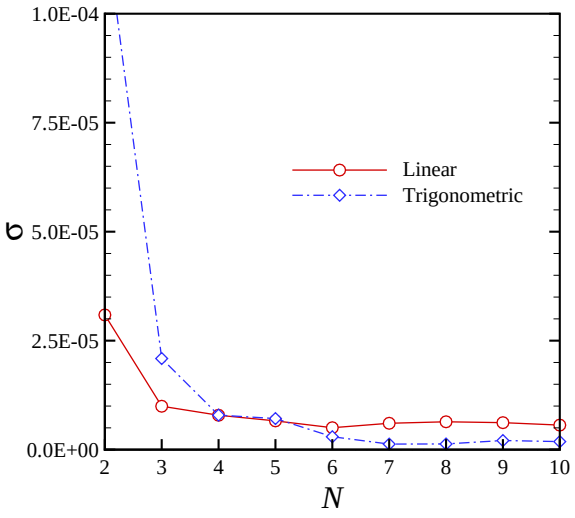

Figure 2: Root mean square difference σ between B-splines curves generated with increasing number of control points and the geometry provided by the MOC. The linear and trigonometric distributions correspond to Eq. 1 and 2 respectively.

2.2 Optimization process

The aim of the optimization process is to quantify the influence of a nozzle length reduction on a) the uniformity of the Mach number and b) the flow angle, both along the nozzle outlet boundary. This is quantified by means of three different objective functions φ. The first function φ_L is simply the inverse of the throat span since it is related to the

nozzle length. The other two functions are a measure of the uniformity of the discharge flow. In particular, φ_M and φ_α are the root mean square deviation of the local Mach number with respect to the design one and the root mean square of the local discharge flow angle, respectively. All objective functions have to be minimized. To summarize, the multi-objective optimization problem statement reads

$$\begin{aligned} \min \quad \varphi_L &= \frac{1}{S_t}\,, \\ \min \quad \varphi_M &= \sqrt{\frac{1}{q}\sum_{j=1}^{q}\left(M_j - M_{\text{req}}\right)^2}\,, \\ \min \quad \varphi_\alpha &= \sqrt{\frac{1}{q}\sum_{j=1}^{q}\arctan^2\left(\frac{M_{y,j}}{M_{x,j}}\right)}\,, \end{aligned} \tag{3}$$

where M_j is the Mach number of the j-th cell and $M_{x,j}$ and $M_{y,i}$ are the Mach numbers obtained by considering only the x and y component of the velocity vector, respectively. All these quantities are evaluated at the outlet boundary discretized by q nodes; M_{req} is the prescribed discharge Mach number and S_t is the throat span.

Evolutionary algorithms and gradient-based methods are the most widely used strategies to solve optimization problems. If the objective is single, gradient-based methods are very efficient; however, they can converge to local minima. In the case of multi-objective optimization, moreover, due to the complexity of the problem, gradient-based methods are often impossible to be used. Differently, evolutionary algorithms such as evolution strategies and Genetic Algorithms[11,12] (GAs) are robust, flexible and easy to implement because they require only the evaluation of the objective functions for a given set of design variables. GAs are global optimization methods able to find the proximity of the global optimum even if the objective function features local optima. Due to the population-based approach, however, GAs require a large number of objective function evaluations, which is a drawback particularly if the evaluations require computationally intensive fluid dynamic simulations.

In this work, the optimization problem is performed by the Multi-objective Genetic Algorithm (MOGA-II),[13,14] which is implemented in the *modeFRONTIER*[15] optimization environment. The algorithm requires a very limited number of user-defined parameters, which in this study have been set to their default values.

2.3 Grid generation and flow-field computation

An automated 2D structured mesh generator based on the solution of an elliptic partial differential problem has been used to build the computational grids for all the geometries tested during the optimization process. An example of a mesh is shown in Figure 3. Two conflicting requirements must be considered when deciding the number of grid points.

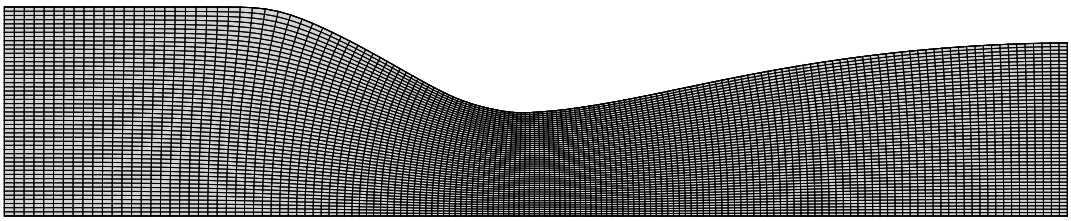

Figure 3: Example of grid generated during the optimization process (150x50 cells).

On one hand, since the optimization technique requires a large number of simulations (in the order of hundreds), it is recommended to keep the number of grid nodes low to reduce the computational cost for each simulation. On the other hand, the accuracy of the computed flow field is proportional to the number of grid cells. Therefore, in order to achieve a compromise between accuracy and computational speed, a grid convergence study has been performed. Figure 4, shows the results obtained by meshes with increasing number of grid nodes. The considered geometry is that obtained by the MOC. Note that due to discretization errors in MOC computations, the exit Mach number M_x and M_y are not identically 2 and 0, respectively, as required by the design constraints. According to these results, a grid of 150x50 nodes in the axial and span-wise direction is adopted in the following since no significant improvement in accuracy is obtained by using finer grids. The numerical solutions of the two-dimensional Euler equations are computed with the

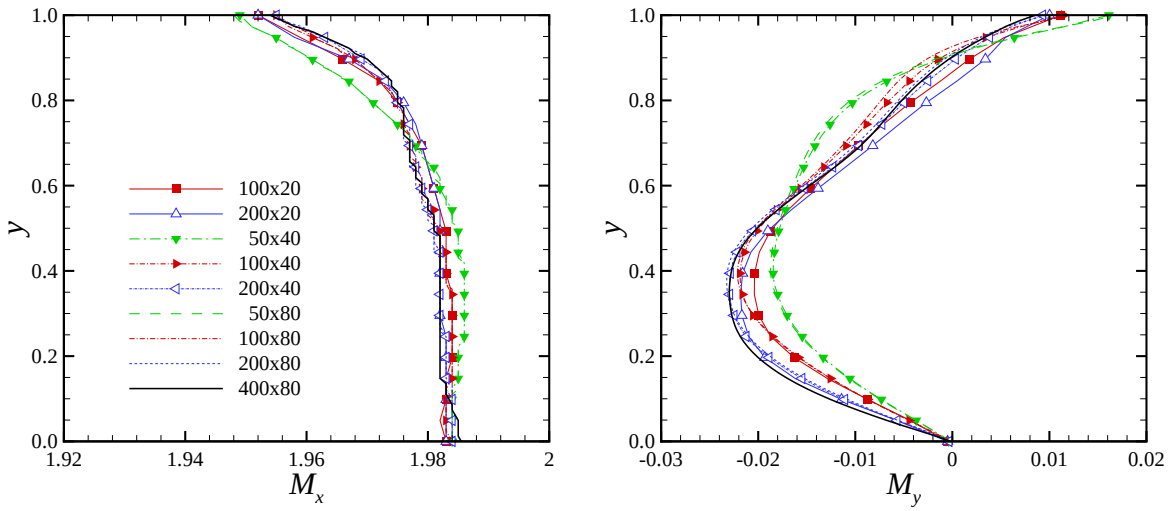

Figure 4: Influence of the number of cell nodes on the Mach number at the discharge section. The distribution of the M_x and M_y components are shown in the left and right plot respectively.

zFlow program.[16–19] The solver uses a hybrid Finite Element (FE)/Finite Volume (FV)

approach in which the finite volume metric quantities are computed using the standard linear Lagrange polynomials basis functions of the finite element method.[20] The spatial approximation of the inviscid flow equations is constructed with a high resolution finite volume method suitable for general unstructured and hybrid grids; the first order scheme is the well-known Roe approximate Riemann solver.[21] This class of discretization schemes is particularly well suited to the computation of high Mach number flows.

zFlow adopts an implicit time integration scheme, which computes steady state solutions in a much more efficient way with respect to conventional explicit schemes. The zFlow solver has been successfully validated for ideal-gas simulations.[16,17] zFlow is linked to a fluid property library containing several thermodynamic models[22] and a large set of fluid data. In this study, the thermodynamic properties of nitrogen are calculated using the polytropic ideal gas law with ratio of specific heats $\gamma = 1.39$.

At the inflow, the stagnation state and the flow angle are prescribed. At the outlet no boundary conditions are needed for a supersonic flow. Slip and symmetry conditions are applied for the nozzle wall and nozzle centerline, respectively.

The solutions are advance in time until the L^2-norm of the residuals are reduced to 10^{-6} times with respect to the first iteration.

3 RESULTS

A Multi-objective Optimization Problem (MOP) can be defined as the problem of finding a vector of design variables $\mathbf{v}_i$ which satisfies a given set of constraints and optimizes a vector of functions whose elements represent the objective functions φ_i. A vector $\mathbf{v}_i$ is considered Pareto optimal if there exists no other feasible vector of design variables which would decrease any of the objective functions, without causing a simultaneous increase in at least another one. Since objective functions are very often competitive, the solution of a MOP is a set of vectors called the Pareto optimal set which represent a trade-off between of the objectives. The plot of the objective functions, whose vectors $\mathbf{v}_i$ are in the Pareto optimal set, is called the Pareto front. In the present work, a set of control points which determines a diverging nozzle shape as defined in Section 2.1 represent a vector of design variables and the objective functions φ are described in Eq. 3. Furthermore, thanks to the scale independence of the present inviscid computations, the nozzle length is expressed in throat span units.

In Figure 5(a), all CFD computations generated by the GA are plotted in a three-dimensional space spanned by the objective functions. In Figure 5(b) only the solutions constituting the Pareto optimal set, which represents a trade-off between nozzle length and flow uniformity, are shown. In these figures, the numerical solution computed over the geometry provided by the MOC procedure (red diamond) is also shown. As mentioned above, due to discretization errors during the MOC computations, this solution lies behind the Pareto front and, for approximatively the same nozzle length, there are better shapes in both flow uniformity terms φ_M and φ_α. Moreover, since the MOC procedure can be adopted to design only the diverging part of the nozzle, the assumptions made for the

sonic line shape are no longer valid because in a CFD computation the flow solution depends on the entire geometry, thus explaining the differences between the CFD and the MOC results.

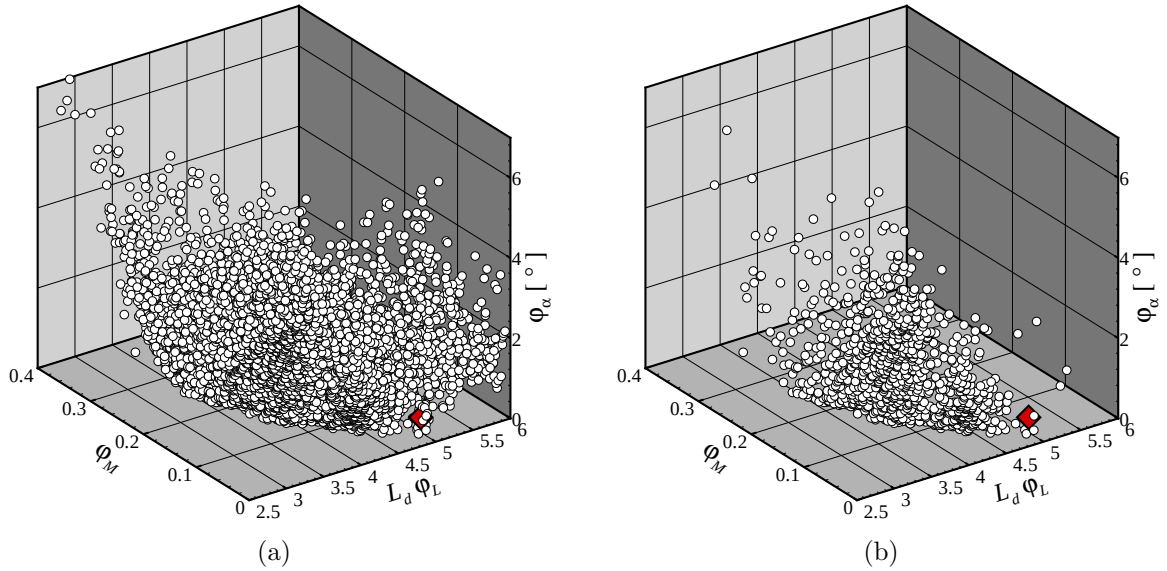

Figure 5: a) All CFD computations generated by the genetic algorithm plotted into a three-dimensional space spanned by the objective functions. b)Discrete surface build by Pareto optimal solutions. The red diamond represents the CFD solution computed over the MOC geometry.

The influence of the length on the discharge Mach number and flow angle are now discussed separately. For this purpose, a two-dimensional Pareto front relating two objective functions is extracted by selecting a suitable constant value for the third objective function. This Pareto front corresponds to the trade-off between the remaining objective functions. Since the Pareto front is build by discrete points, one objective function has to be fixed to a small range centered on the desired value to include a group of points which lie in the proximity.

In Figure 7(a), four trade-off between Mach number deviation and nozzle length for different values of discharge angle are shown. Similarly, Figure 7(b) shows the trade-off between the outlet flow angle and the nozzle length for fixed values of the Mach number deviation.

In Table 1 different values of the objective functions for the MOC shape and Pareto optimal designs, i.e., D1, D2 and D3, are compared. The first design, D1, is an optimal solution with approximatively the same nozzle length of the MOC Geometry. The second and third solutions, D2 and D3 , minimizing the nozzle length, are opposite trade-off in terms of φ_M and φ_α respectively.

For these four selected design, Figures 7(a) and 7(b) show the local distributions of the Mach number deviation and local flow angle along the discharge section. For the same

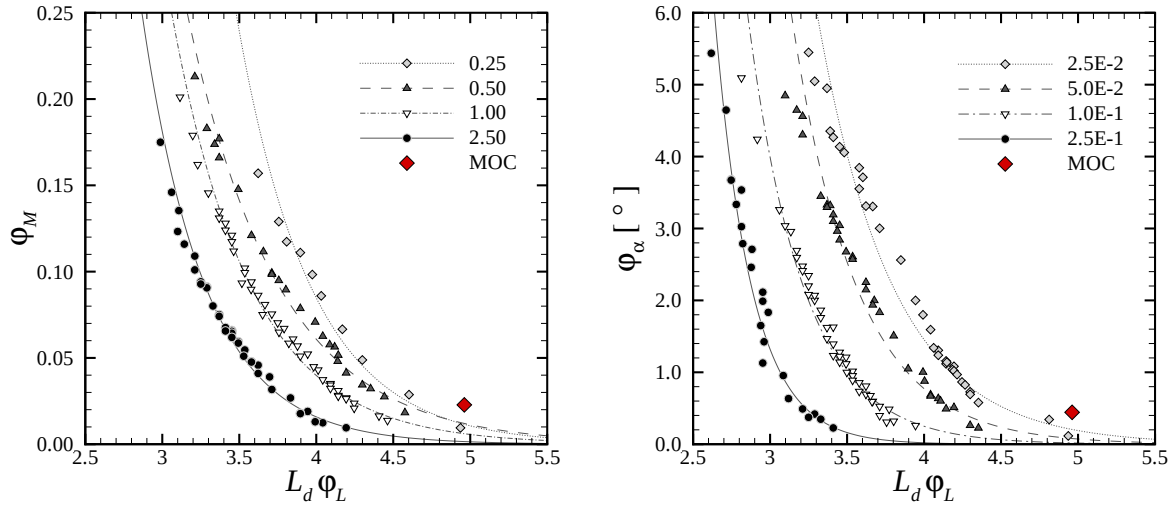

(a) (b)

Figure 6: a) Trade-off between the deviation of the Mach number φ_M and nozzle length $L_d\varphi_L$ for different values of the discharge flow angle, i.e., $\varphi_\alpha \cong 2.5 \cdot 10^{-2}, 5.0 \cdot 10^{-2}, 1.0 \cdot 10^{-1}$ and $2.5 \cdot 10^{-1}$. b) Trade-off between flow angle φ_α and nozzle length $L_d\varphi_L$ for different values of the of the Mach number deviation, i.e., $\varphi_M \cong 2.5 \cdot 10^{-1}, 5.0 \cdot 10^{-1}, 1$ and 5 degrees. For each trade-off an interpolating line is show.

geometries, Mach number contours and nozzle shapes are shown in Figure 8.

Among the four considered designs, design D1 is that closer to the MOC design and indeed it presents the smallest deviation from design constraints in terms of Mach uniformity and zero velocity angle at the exit section. The length is very close to the MOC one. In design D2, instead, the shortest nozzle among the four considered is obtained. The Mach number is almost uniform at the exit by the average velocity angle is as large as 5°. The nozzle length is about 77% of the reference one. In design D3, trade-off between Mach number uniformity and nozzle length is more clear. A reduction of about 16% of the nozzle length is achieved by letting the average Mach number at the exit section depart as much as 5% from the design value.

Table 1: Comparison between MOC geometry and selected examples of reduced length nozzles in terms of objective function values.

Design	$L_d\varphi_L$	φ_M	φ_α [°]
MOC	4.961	$2.279 \cdot 10^{-2}$	$4.433 \cdot 10^{-1}$
D1	4.467	$2.215 \cdot 10^{-2}$	$4.406 \cdot 10^{-1}$
D2	3.802	$3.523 \cdot 10^{-2}$	2.022
D3	4.143	$5.161 \cdot 10^{-2}$	$4.916 \cdot 10^{-1}$

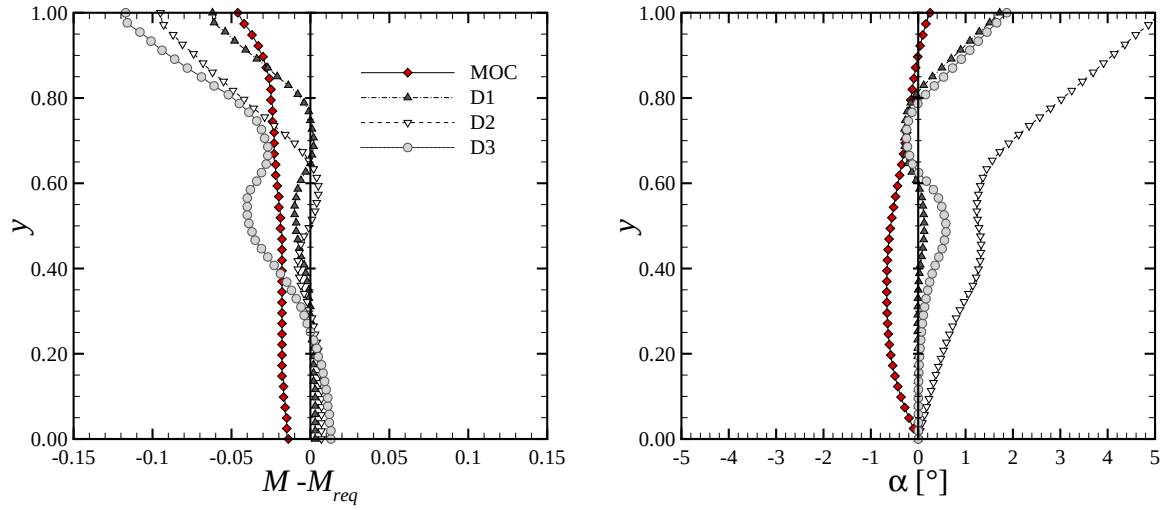

Figure 7: Distributions of the Mach number deviation with respect to the requested one (a) and local flow angle (b) along the discharge section corresponding to the solutions of Table 1.

4 CONCLUSIONS

For a supersonic nozzle of rectangular cross-sectional area, the influence of a nozzle length reduction on the uniformity of the Mach number and the flow angle, both along the nozzle outlet boundary, is investigated. In contrast to the results obtained from the standard Method of Characteristics (MOC), which yields only one single design and no information regarding sensitivities, the investigation presented is based on a multi-objective optimization procedure employing a Genetic Algorithm and a parameterization of the shape of the diverging part of the nozzle wall using cubic B-spline curves. The grid is generated using an automated 2D mesh generator and the numerical solutions of the two-dimensional Euler equations are computed with the zFlow flow solver.

The resulting Pareto set of optimal nozzle shapes shows that, for approximatively the same nozzle length of the design obtained using the MOC approach, there exist better nozzle shapes in terms of flow uniformity at the required discharge Mach number. This improvement is possibly due to discretization errors in MOC computations and to the possibility of changing the nozzle curvature at the nozzle throat section, whereas in MOC computations this quantity is fixed. Many optimal solutions show also interesting trade-off between nozzle length and flow uniformity. For the design of high-quality supersonic nozzles, the optimization approach is the preferred method as opposed to the MOC approach. Moreover, the optimization approach can be easily extended to allow for the complete viscous design of nozzles, taking into account viscous effect such as boundary layers growth and the influence of the converging nozzle section upstream of the throat that features subsonic flow.

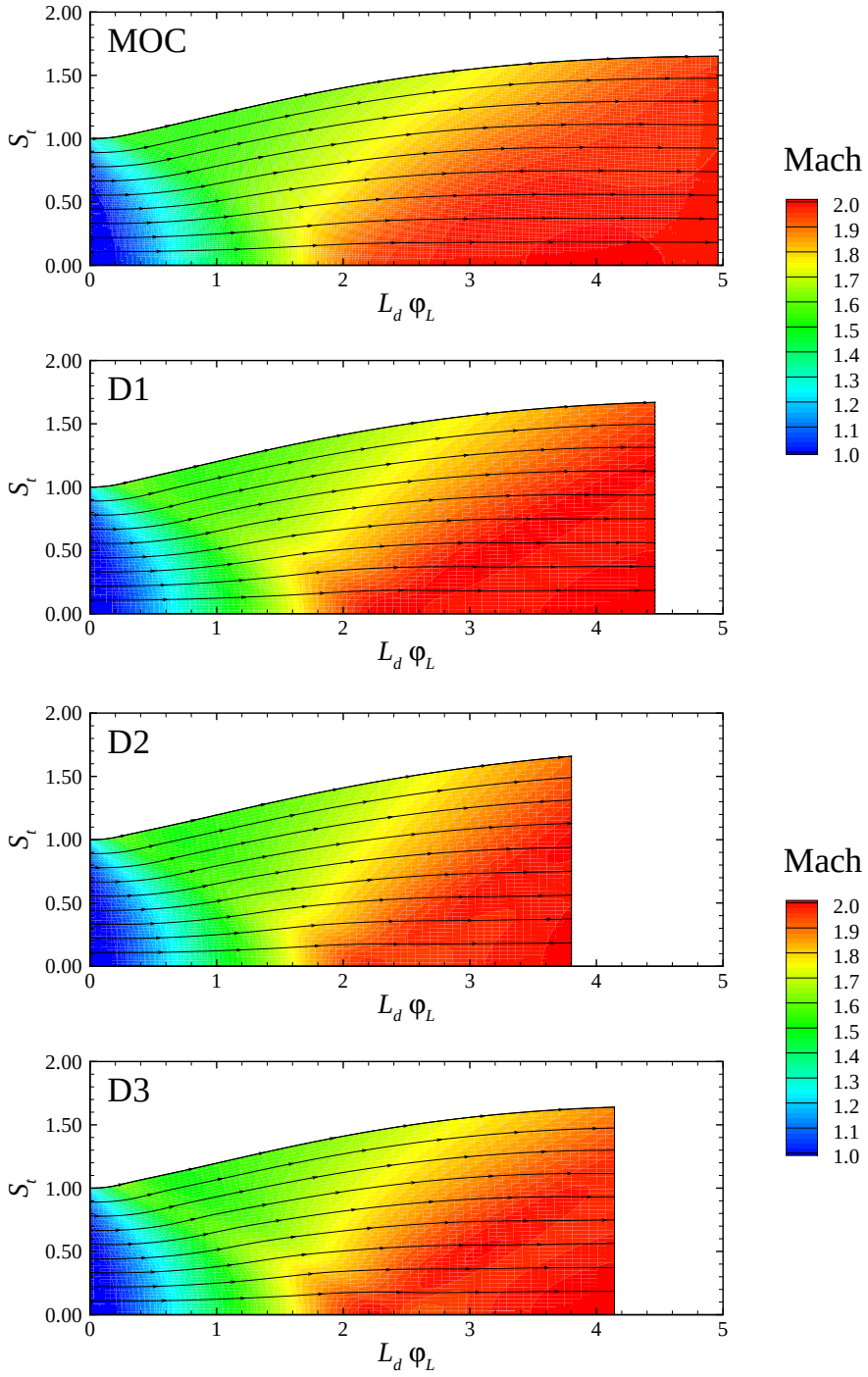

Figure 8: Difference in terms of nozzle shape and Mach number contours between the solution obtained by the MOC procedure and three examples of Pareto optimal designs, i.e., D1, D2 and D3.

REFERENCES

[1] G. Sutton and O. Biblarz. *Rocket Propulsion Elements*. John & Sons, Inc., 2001.

[2] J. Harinck, T. Turunen-Saaresti, P. Colonna, and J. van Buijtenen. Computational study of a high-expansion ratio radial ORC turbine stator. *J. Eng. Gas Turb. Power*, 2009. Accepted for Publication.

[3] J.J. Korte. Inviscid design of hypersonic wind tunnel nozzles for real gas. In *E. Camhi, editor, 38th Aerospace Sciences Meeting and Exhibit, Reno, NV, pages 1-8, Reston, VA. AIAA*, Jan. 10-13 2000.

[4] M.J. Zucrow and J.D. Hoffman. *Gas Dynamics, Vol. 2*. Krieger, 1977.

[5] K. Foelsch. The analytical design of an axially symmetric lavalnozzle for a parallel and uniform jet. *Journal of the Aeronautical Sciences*, 16:161–166, 1948.

[6] G. Emanuel and B.M. Argrow. Comparison of minimum length nozzles. *Journal of Fluid Engineering – Trans. ASME*, 110:283–288, 1988.

[7] A. C. Aldo and B. M. Argrow. Dense gas flow in minimum length nozzles. *J. Fluids Eng.*, 117:270–276, 1994.

[8] G. Farin. *Curves and Surfaces for Computer Aided Geometric Design*. Academic Press, San Diego, CA, 4^{th} edition, 1997.

[9] L. Piegl and W. Tiller. *The NURBS Book*. Springer-Verlag, 1995.

[10] J. Hoschek, D. Lasser, and L.L. Schumaker. *Fundamentals of Computer Aided Geometric Design*. A. K. Peters, Ltd., Natick, MA, 1993.

[11] David E. Goldberg. *Genetic Algorithms in Search, Optimization and Machine Learning*. Addison-Wesley Longman Publishing Co., Inc., Boston, MA, 1989.

[12] J. Periaux and H. Deconinck, editors. *Introduction to Optimization Methods and Tools for Multidisciplinary Design in Aeronautics and Turbomachinery*, VKI Lecture Series LS 2008-07. von Karman Institute for Fluid Dynamics, June 2008.

[13] C. Poloni and V. Pediroda. *Genetic Algorithms and Evolution Strategies in Engineering and Computer Science*, chapter GA coupled with computationally expensive simulations: tools to improve efficiency., page 267288. John Wiley and Sons, England, 1997.

[14] S. Poles. MOGA-II an improved multi-objective genetic algorithm. Technical Report 003-006, ESTECO, Trieste, Italy, 2003.

[15] *modeFRONTIER 4.0, ESTECO srl, modeFRONTIER User Manual*.

[16] P. Colonna and S. Rebay. Numerical simulation of dense gas flows on unstructured grids with an implicit high resolution upwind Euler solver. *Int. J. Num. Meth. Fluids*, 46:735–765, 2004.

[17] P. Colonna, A. Guardone, J. Harinck, and S. Rebay. Numerical investigation of dense gas effects in turbine cascades. In *15^{th} U.S. National Congress on Theoretical and Applied Mechanics Conference, Boulder, CO*, 2006.

[18] P. Colonna, S. Rebay, J. Harinck, and A. Guardone. Real-gas effects in ORC turbine flow simulations: influence of thermodynamic models on flow fields and performance parameters. In *ECCOMAS CFD 2006 Conference, Egmond aan Zee, NL*, 2006.

[19] P. Colonna, J. Harinck, S. Rebay, and A. Guardone. Real-gas effects in organic rankine cycle turbine nozzles. *AIAA Journal of Propulsion and Power*, 24(2):282–294, 2008.

[20] V. Selmin. The node-centered finite volume approach: bridge between finite differences and finite elements. *Computer Methods in Applied Mechanics and Engineering*, 102(1):107–138, 1993.

[21] P. L. Roe. Approximate Riemann solvers, parameter vectors, and difference schemes. *Journal of Computational Physics*, 43(2):357–372, 1981.

[22] P. Colonna, T. P. van der Stelt, and A. Guardone. FluidProp: A program for the estimation of thermophysical properties of fluids. Software, 2004.